Published in final edited form as:
Bioconjug Chem. 2010 December 15; 21(12): 2305–2312. doi:10.1021/bc100336b.

Improved Speciation Characteristics of PEGylated Indocyanine Green-Labeled Panitumumab: Revisiting the Solution and Spectroscopic Properties of a Near-Infrared Emitting anti-HER1 Antibody for Optical Imaging of Cancer

Aaron Joseph L. Villaraza, **Diane E. Milenic**, and **Martin W. Brechbiel***
Radioimmune and Inorganic Chemistry Section, Radiation Oncology Branch, National Cancer Institute, National Institutes of Health, 10 Center Drive, Bethesda, Maryland 20892-1002

Abstract

A water-soluble amine-reactive PEGylated analogue of near-infrared emitting dye indocyanine green (**5**) was synthesized and used to label the anti-HER1 antibody panitumumab (Vectibix) at various equivalents. These conjugates were compared with non-PEGylated analogue conjugate products and the solution speciation analyzed with UV-Vis spectrophotometry, size exclusion HPLC and SDS-PAGE. PEGylation of the bioconjugates was successful in preventing aggregation in solution, a phenomenon observed with the non-PEGylated bioconjugates presumably due to the hydrophobicity of indocyanine green. Competitive radioimmunoassay demonstrated that the targeting moiety of the PEGylated bioconjugates was conserved. Fluorescence microscopy also demonstrated membrane binding of the bioconjugate to HER1-expressing A431 cells. Hence, these bioconjugates are suitable candidates for the *in vivo* optical imaging of HER1-expressing tumors.

Introduction

There has been a great amount of interest in near-infrared (NIR) dyes as reporter groups for bioconjugate probes as NIR light (700–1000 nm) is relatively transparent to tissue (1). The many applications of NIR dyes for *in vivo* fluorescence biological imaging has been reviewed in detail elsewhere (2–3). Chief among this class of reporter groups are the water-soluble cyanine (Cy) dyes designed to react selectively with either sulfhydryl or amine groups present on biomolecules (4–8).

However, excessive loading of Cy dye on proteins results in quenching of fluorescence, a phenomenon more pronounced in the longer-chain cyanine dyes, such as Cy5 and Cy7 (9). Indeed, dye-dye-mediated self-quenching was found to be more evident in the Cy dyes than in other commercially available NIR dyes, such as the AlexaFluor dyes (10). This phenomenon has led to the development of particular applications such as enzyme-responsive NIR-protein bioconjugates which fluoresce upon enzymatic cleavage of the bioconjugate (11–13). Cy dyes have also been used to label monoclonal antibodies (mAbs) targeting tumor-associated antigens (14–17), with Cy7 demonstrating a fluorescence

*To whom correspondence should be addressed: Martin W. Brechbiel, PhD. Radioimmune and Inorganic Chemistry Section, Radiation Oncology Branch, NCI, NIH, 10 Center Drive, Building 10, Room B3B69, Bethesda, Maryland 20892-1002. Phone: (301) 496-0591. Fax: (301) 402-1923. martinwb@mail.nih.gov.

Supporting Information Available: NMR spectra of compounds **4** and **5**, and *in vitro* confocal microscopy images of compounds **12** and **15** with viable A431 cells are presented. This information is available free of charge via the Internet at http://pubs.acs.org/.

response with the deepest tissue penetration (14). More recently, mAbs labeled with both a Cy dye and a radioactive reporter have been described towards the development of multi-modal diagnostic agents (18–19).

Indocyanine green (ICG) (**1**) is an FDA-approved cyanine dye first described in the construction of dilution curves for cardiovascular physiological studies (20). The absorption and emission characteristics of this dye at the near-infrared end of the spectrum further extended its application to fluorescence angiography (21), necessitating a thorough investigation of the effects of solvent on the absorption and emission spectra of ICG in blood plasma in comparison with ICG dissolved in commonly used laboratory solvents (22–23). In general, it has been observed that dye-aggregation, whether due to the nature of the solvent, the concentration of the dye, or combinations of both, results in the quenching of ICG fluorescence.

Monoclonal antibody conjugates with amine-reactive ICG (24–25) (**2** and **3**) (Figure 1) have been used in immunohistochemical staining of gastric microcancers (26–29) and as an *in vivo* probe for tumor imaging (30–32). Interestingly, some examples of these ICG-mAb bioconjugates were found to be non-fluorescent in PBS, but became fluorescent either *in vitro* when in the presence of denaturing agents such as 5% SDS and β-mercaptoethanol (β-ME), or upon internalization in tumor cells (31–32). The exact mechanism for this observed fluorescence activation was not elucidated, though the authors suggest aggregation as the cause of fluorescence quenching. Furthermore, these conjugates also exhibited significant uptake and retention in the liver.

The studies herein describe an amine-reactive PEGylated ICG analogue (**5**) and its conjugation to the mAb panitumumab. Panitumumab (Vectibix) is an FDA-approved mAb which binds to HER1 (33), a surface antigen which is over-expressed in a variety of cancers. These conjugates were compared with mAb conjugates of non-PEGylated analogues **2** and **3**, their solution speciation characterized spectroscopically and chromatographically. The immunoreactivity of the mAb post-modification was evaluated by radioimmunoassay using purified antigen and by fluorescence microscopy. PEGylation was found to render ICG water-soluble, thereby obviating the need for intermediary solvents such as DMSO or DMF in the conjugation reaction. The PEGylated ICG-mAb was hypothesized to exhibit improved solubility and pharmacokinetic characteristics, and to minimize or eliminate aggregation of the conjugation product in comparison with the non-PEGylated analogue. Furthermore, PEGylation of biologically active molecules, antibodies and antibody fragments has been found to reduce their immunogenicity and improve *in vivo* clearance (34–35).

Materials and Methods

Compounds **2** and **3** were synthesized as previously described (24–25). NH_2-PEG-CM-3400 (average molecular weight 3250) was purchased from Laysan Bio Inc. (Arab, AL). 1-Ethyl-3-(3-dimethylaminopropyl)carbodiimide hydrochloride (EDC) and 2-mercaptothiazoline (ATT) were obtained from TCI America (Portland, OR) and 4-dimethylaminopyridine (DMAP) was purchased from Sigma-Aldrich Chemical Company (St. Louis, MO). Sephadex G-25 Medium was purchased from GE Healthcare (Piscataway, NJ). Panitumumab (AMGEN Inc., Thousand Oaks, CA) was purchased through the Veterinary Resources Pharmacy, NIH.

^{1}H and ^{13}C NMR spectra were obtained using a Bruker Avance 300 MHz instrument and chemical shifts are reported in ppm on the δ scale relative to TMS or residual solvent. Proton chemical shifts are annotated as follows: ppm (multiplicity, coupling constant (Hz),

integration). Reaction progress was also monitored by Silica Gel 60 thin layer chromatography (Merck, Germany).

Absorbance spectra were recorded on an Agilent 8453 spectrophotometer (Santa Clara, CA). Size exclusion HPLC (SE-HPLC) was performed on a Waters HPLC system (Milford, MA) using a TOSOH TSK4000SW column (Tokyo, Japan) with 67 mM Na_3PO_4/100 mM KCl buffer (pH 6.8) as eluent (flow rate 0.5 mL/min). Radioactivity was measured using a Wizard One Perkin Elmer γ-scintillation counter (Shelton, CT).

ICG-PEG-COOH (4)

NH_2-PEG-CM-3400 (1.0 g, 0.31 mmol) was dissolved in MeCN (50 mL) and stirred in the presence of Et_3N (50 μL, 0.36 mmol) over ice. Compound **3** (0.24 g, 0.34 mmol) was added, and the solution stirred over ice for 1 h and 18 h at room temperature. The reaction mixture was diluted with $CHCl_3$ (50 mL) and washed with 0.1 M HCl (50 mL). The aqueous layer was extracted further with $CHCl_3$ (2 × 50 mL). The organic portions were pooled together and dried over anhydrous $MgSO_4$. The mixture was filtered and the filtrate evaporated under reduced pressure. The dye-polymer conjugate was purified by passing through a Sephadex G-25 size exclusion column previously equilibrated with water. The volume of the pure fraction was brought up to ~50 mL with water, acidified with 0.1 M HCl, and extracted into $CHCl_3$ (3 × 50 mL). The organic portions were pooled together, dried over anhydrous $MgSO_4$, filtered, and the filtrate evaporated under reduced pressure. The dark green oily residue was triturated with diethyl ether, the supernatant decanted, the resulting solid washed with more diethyl ether, and the residue dried under reduced pressure to yield a dark green powder (0.91 g, 77%). R_f = 0.5 ($CHCl_3$:MeOH::9:1); ^{1}H NMR ($CDCl_3$, 300 MHz) δ 1.5 (t, *J* = 7.2 Hz, 3H), 1.6–2.4 (m, 6H), 2.0 (s, 12H), 3.4–3.5 (m, 5H), 3.6–3.8 (m, 307H), 3.9 (t, *J* = 6.2 Hz, 3H), 4.1–4.4 (m, 4H), 4.2 (s, 2H), 6.3 (d, *J* = 13.1 Hz, 1H), 6.4 (d, *J* = 12.9 Hz, 1H), 6.8 (m, 2H), 7.3–8.2 (m, 15H); ^{13}C NMR ($CDCl_3$, 300 MHz) δ12.74, 25.22, 26.50, 27.58, 36.15, 39.08, 44.66, 50.90, 59.53, 68.97, 69.72, 70.23, 71.27, 81.61, 110.09, 110.56, 122.18, 124.81, 124.99, 127.70, 128.20, 128.33, 130.00, 130.55, 130.66, 131.63, 131.78, 133.54, 133.75, 139.25, 139.53, 171.42, 173.08; λ_{max} = 783 nm (PBS).

ICG-PEG-ATT (5)

Compounds **4** (0.76 g, 0.20 mmol) was dissolved in DCM (20 mL) and cooled over ice. EDC (45 mg, 0.22 mmol) and DMAP (27 mg, 0.22 mmol) were added and the solution stirred for 30 min. Afterwards, ATT (26 mg, 0.22 mmol) was added, and the reaction was stirred over ice for 1 h and at room temperature for 18 h. The reaction mixture was then washed successively with 0.1 M $NaHCO_3$ (1 × 50 mL) and 0.1 M HCl (2 × 50 mL). The organic portions were pooled together, dried over anhydrous $MgSO_4$, filtered, and the filtrate evaporated under reduced pressure. In a similar manner as with **4**, the residue was triturated with diethyl ether and then dried under reduced pressure to yield a dark green powder (0.64 g, 84%). R_f = 0.8 ($CHCl_3$:MeOH::9:1); ^{1}H NMR ($CDCl_3$, 300 MHz) δ 1.5 (t, *J* = 7.0 Hz, 3H), 1.6–2.4 (m, 6H), 2.0 (s, 12H), 3.4–3.5 (m, 5H), 3.6–3.8 (m, 295H), 3.9 (m, 3H), 4.0 (t, J = 7.8 Hz, 2H), 4.1–4.4 (m, 4H), 4.6 (t, *J* = 7.2 Hz, 2H), 5.1 (s, 2H), 6.3 (d, *J* = 13.1 Hz, 1H), 6.4 (d, *J* = 12.9 Hz, 1H), 6.8 (m, 2H), 7.3–8.2 (m, 15H); ^{13}C NMR ($CDCl_3$, 300 MHz) δ 12.78, 25.27, 26.44, 27.61, 29.56, 33.75, 36.19, 39.12, 44.68, 50.92, 51.60, 55.48, 59.50, 60.00, 70.54, 74.00. 81.58, 110.16, 110.67, 122.22, 125.07, 127.77, 128.21, 130.03, 130.62, 131.64, 133.48, 133.71, 139.22, 139.51, 171.97, 173.12, 201.13; λ_{max} = 783 nm (PBS).

Conjugation of Antibodies

Solutions of mAb (typically 10 mg, 66.7 nmol) were incubated with 2, 4, or 8 equivalents of **2**, **3** or **5** in 0.1 M $NaHCO_3$ (pH 8.5) buffer for 1 h at 37 °C with stirring at 750 rpm. The

mAb solution was vortexed as the amine-reactive dye was added dropwise to ensure homogeneity of the reaction. All conjugation reactions were made up to a total volume of 1 mL. In particular, **5** was added as a 200 μL aliquot in buffer, while **2** and **3** were added as a 200 μL aliquot in DMSO. After incubation, the reaction was transferred to a 3 mL Slide-A-Lyzer Dialysis Cassette G2 (Thermo Fisher Scientific, Rockford, IL) and dialyzed against PBS buffer at 4 °C for three days with nine buffer changes (9 L total). Protein recovery during conjugation was determined by measuring the UV absorption at 280 nm.

Absorbance Measurements

The extinction coefficient of **3** was determined in DMF and in 9:1 PBS:DMF solution, while the extinction coefficient of **5** was determined in DMF, in 9:1 PBS:DMF solution, and in PBS. The absorbance spectra of 50 μg/mL samples of the bioconjugates were measured in PBS and in 9:1 PBS/DMF. Based on a previously described procedure (22), the changes in the shape of the spectra as a function of concentration were monitored by preparing 500, 100, 50 and 10 μg/mL samples of bioconjugate. The absorbance spectra of 500 μg/mL and 50 μg/mL samples were measured in a 2 mm cuvette, while 100μg/mL and 10 μg/mL samples were measured in a 10 mm cuvette. The spectra of samples whose product of concentration *c* and pathlength *b* were the same (i.e. $A = \varepsilon bc$ where bc = constant) where superimposed. These measurements were performed in PBS and in 8:2 PBS:DMSO.

Competition Radioimmunoassay (General Procedure)

The immunoreactivities of immunoconjugates were evaluated using a competition radioimmunoassay. Fifty (50) ng of human epidermal growth factor receptor (hEGFR) (Sigma-Aldrich, St. Louis, MO) in 50 μL of PBS containing Mg^{2+} and Ca^{2+} was added to each well of a 96-well plate and incubated overnight at 4 °C. The excess antigen was removed, 150 μL of 1% bovine serum albumin in PBS (BSA/PBS) was added to each well, and the plate allowed to sit at ambient temperature for 1 h. The wells were then aspirated and serial dilutions (1000–0.02 ng in 50 μL BSA/PBS) of the immunoconjugates were added to the wells in triplicate (leaving one set of wells as a blank, i.e. no competitor), followed by ^{125}I-panitumumab (36) (~50,000 cpm in 50 μL BSA/PBS). The plate was then incubated at 37 °C for 4 h. Afterwards, the wells were emptied and washed with BSA/PBS (3 × 200 μL), the bound radioactivity removed with 100 μL 0.2 M NaOH, absorbed into cotton filters, placed in 12 × 75 mm tubes and counted in a γ-scintillation counter. The percent inhibition was calculated and plotted. Unconjugated panitumumab was included in the assay as well as a negative mAb HuM195 (kindly provided by M. McDevitt, Memorial Sloan Kettering Cancer Center), which reacts with human CD33.

SDS-Polyacrylamide Gel Electrophoresis

The immunoconjugates were analyzed by SDS-polyacrylamide gel electrophoresis (SDS-PAGE) both with and without reduction by β-ME using 4–20% pre-cast Tris-Glycine polyacrylamide gels, respectively (Invitrogen, Carlsbad, CA). Five (5) μg of the immunoconjugates were added to each lane and the gels were run according to the method of Laemmli (37). Lanes containing 5 μg of panitumumab were included as a comparison.

Fluoresence microscopy

HER1-positive A431 cells were utilized for fluorescence microscopy to demonstrate tumor targeting and specificity of the PEGylated panitumumab-ICG conjugate. The cells were obtained from ATCC (Manasass, VA) and grown in RPMI 1640 media (Lonza, Walkersville, MD) supplemented with 10% FetalPlex (Gemini Bioproducts, Woodland, CA), 1 mM non-essential amino acids and 2 mM glutamine. The fluorescence microscopy study was performed by adding A431 cells (2.5×10^4) to each chamber of an eight chamber

slide and incubated for 72 h. The chambers were washed 3 times with phosphate-buffered saline (PBS, pH 7.2) and fixed for 10 min at room temperature with 4% paraformaldehyde. After three more washes with PBS, 0.5 mL of PBS containing 1% bovine serum albumin was added to each chamber. Following 1 h incubation at ambient temperature, the 1% BSA/PBS was removed and 1 μg of **12** or **15** (negative control) was added to a chamber and incubated for 1 h at 37 °C. The chambers were then washed three times with PBS, the chambers removed and the slide mounted with a coverslip using FluorSave (Calbiochem, La Jolla, CA). Fluorescence microscopy was performed using an Olympus BX61 microscope (Olympus America, Inc, Center Valley, PA) equipped with the following filters: excitation wavelength 672.5 to 747.5 nm, emission wavelength 765 to 855 nm. Transmitted differential interference contrast (DIC) images were also collected.

Results and Discussion

Amine-reactive ICG dyes **2** and **3** were synthesized in good yields. To produce ICG-PEG conjugate **4**, compound **2** was chosen to react with NH_2-PEG-CM-3400 as the aminolysis of 3-acylthiazolidine-2-thione activated esters to form amides has been thoroughly demonstrated to be efficient (38–39). Furthermore, the reactivity of **2** itself has been tested with a variety of amino acids and primary amines under different conditions and found to be efficient (25). The benefits of PEGylating ICG were expected to be three-fold: firstly, the dye-polymer conjugate **4** would be dramatically more water-soluble than **2**; secondly, the increase in molecular weight would promote simplified purification of the resulting dye-polymer conjugate **4** by size-exclusion chromatography (indeed, due to the differences in molecular weight and solubility between the starting materials and product, unreacted dye was retained at the top of the Sephadex column while the dye-polymer eluted); thirdly, since the molecular weight of the polymer is significantly greater than that of the dye, the resulting mass of **4** is much higher relative to the amount of **2** used in the reaction, which again facilitates handling. This bodes well if the same reaction scheme is to be applied to the synthesis of dye-polymer conjugates using commercially-available Cy dyes, which are relatively expensive and sold only in small amounts. Interestingly, **4** could, in fact, be extracted back into chloroform upon slight acidification of the purified fraction. Synthesis of activated ester **5** was chosen over a succinimidyl ester analogue in order to be able to compare mAb labeling efficiencies with **2** (Scheme 1). The formation of the activated ester was easily monitored by thin layer chromatography. Finally, both PEGylated and non-PEGylated amine-reactive dyes were found to “stick” to the flask, but trituration in diethyl ether dislodged both products, thereby maximizing reaction yields.

Amine-reactive dyes **2**, **3** and **5** were added to panitumumab in increasing equivalents of 2, 4 and 8 per mAb to (1) compare their respective labeling efficiencies and (2) determine the effect of increased labeling on the immunoreactivity of the resulting conjugates (Scheme 2). As **5** proved to be water-soluble, the conjugation reaction was performed solely in buffered aqueous solutions as described above. However, the insolubility of **2** and **3** in aqueous solutions required dissolution in DMSO before addition to the buffered protein solution. Prior to the conjugation reactions with the ICG compounds, the maximum percentage of DMSO in buffer that panitumumab could tolerate without loss of immunoreactivity was determined to be 25% DMSO in reaction buffer (data not shown). Hence, the conjugation reactions involving **2** and **3** were performed with the desired equivalents being added as a 200 μL DMSO solution to 800 μL buffered protein solution, resulting in a final reaction volume of 1 mL. All conjugates were purified via extensive dialysis against PBS and recovered in good yield on a protein basis.

A previous study on the UV-Vis absorption properties of ICG noted that: (1) the characteristics of the absorbance spectrum of ICG are dependent upon its concentration in

solution and the nature of the solvent, (2) at relatively low concentrations the absorbance maximum of the dye is red-shifted when comparing spectra taken in water versus plasma, and (3) a continuous increase in ICG concentration results in a collapse of the absorbance maximum at ~780 nm accompanied by a simultaneous growth of a peak within the range of 700–720 nm (22). The presence of this peak is a clear indication of the formation of dye aggregates in aqueous solvent due to the hydrophobicity of ICG (40). Indeed, analogous solvent- and concentration-dependent formation of dye aggregates has been observed for other cyanine dyes as well (41). The formation of aggregates alters the optical density of the dye, and correspondingly, the extinction coefficient ε. This change has profound implications on the use of ICG as a fluorescent probe in biological applications, as the optical density determines the fluorescence intensity. This occurrence is underlined by the inconsistency of reported ICG quantum yields in the literature, which were also found to be both solvent- and concentration-dependent (23,42).

The extinction coefficients of **3** and **5** were determined in different solvents at micromolar concentrations. Compounds **3** was insoluble in PBS, but soluble in a 10% DMF in PBS solution and in DMF alone. The calculated extinction coefficients were drastically different, being a fifth lower in PBS/DMF than in just DMF. On the other hand, the calculated extinction coefficients of **5** were independent of the three solvents used (Table 1). However, a slight red-shift from 783 nm to 790 nm was observed when comparing the absorbance maxima ranging from aqueous to organic solvent (Figure 2).

More critically, the effect of solvent on the extinction coefficient of the dye has important implications in the determination of the dye-to-protein (D/P) ratio of resulting ICG-labeled proteins. D/P ratios can be determined spectrophotometrically by calculating the concentration of dye based on its absorbance at its λ_{max}, and likewise the protein concentration from its absorbance at 280 nm. These calculations require the construction of a calibration curve for each separate component (i.e., dye and protein) measured in an ideal aqueous solvent such as PBS. As both **3** and **4** are insoluble in PBS, no such calibration curve could be constructed, and therefore D/P ratios for proteins labeled with them cannot be determined. On the other hand, a protein calibration curve in 9:1 PBS:DMF is meaningless as this solvent combination does not mimic physiological conditions. Indeed, in previous reports (31–32) the D/P ratios of a variety of ICG-labeled mAbs were determined under denaturing conditions, i.e., in the presence of 5% SDS and β-mercaptoethanol. Applying the same argument, such results and measurement are at best questionable as these solvent conditions do not reflect the physiological state of the antibody conjugates under study.

However, as the extinction coefficient of **5** is consistent throughout the range of solvents described, the concentrations of panitumumab and ICG can be accurately determined from the absorbances of the conjugates at 280 nm and 783 nm (Figure 3a) in PBS. Using this method, the D/P ratios for the PEGylated dye-protein conjugates **12**, **13** and **14** were calculated to be 0.73, 1.74 and 3.38, respectively. HuM195 was also reacted with **5** to form conjugate **15**, and its D/P ratio was determined to be 1.05. The challenge of determining D/P ratios in dye-labeled proteins is not limited to ICG conjugates; for example, it has been addressed previously in antibody conjugates of rhodamine B, a relatively hydrophobic dye (43–44). The importance of accurately establishing the D/P ratio of a fluorescently-labeled antibody cannot be over-stated as high loading of dye molecules onto a single antibody has been shown to result in fluorescence quenching rather than fluorescence enhancement, observed especially in the longer-chain Cy dyes due to their relative hydrophobicity (9–10).

Absorption spectra of 50 μg/mL samples of all bioconjugates were measured; for brevity, the spectral range corresponding to dye absorption of **8**, **11**, **14** are presented (Figure 3b and

3c). As discussed earlier, the depression of the absorbance peak at 790 nm, the shift and broadening of the λ_{max} to around 800 nm, and the increase of the absorbance within the 700–720 nm range in the spectra of **8** and **11** in PBS are all indicators of dye aggregation in these conjugates, characteristics which are much less pronounced in the spectrum of the PEGylated conjugate **14** (Figure 3b). Similar to previously published absorption spectra of ICG-mAb bioconjugates (27), the spectra of **8**, **11** and **14** when measured in 9:1 PBS:DMF show a suppression of the 720 peak and a growth in the 790 nm peak (Figure 3c) relative to that measured in PBS alone, suggesting that the presence of DMF prevents or reduces dye aggregation. Again, however, this solvent combination is not representative of physiological conditions and therefore absorbance measurements performed in it do not reflect the true absorption properties of these conjugates, particularly when translated to an *in vivo* environment. On the other hand, the absorption spectra of the PEGylated conjugates suggest that they are more stable against dye aggregation, a result of the increased hydrophilicity of **5** due to the water-soluble PEG polymer.

To determine if aggregation is an effect of concentration, the absorption spectrum of **11** was measured at different concentrations (ranging from10 to 500 ng/mL) in PBS (Figures 4a and 4b). Furthermore, to determine if the solvent also had an effect, the same measurements were performed in 20% DMSO in PBS (Figures 4c and 4d). No change was observed in the spectra measured in PBS regardless of the sample concentration. However, for the samples measured in 2:8 DMSO:PBS, the data suggest that aggregation is reduced upon dilution of the sample in the presence of an organic co-solvent, indicated once again by the suppression of the peak at 720 nm and the growth of the peak at 790 nm.

The SE-HPLC data demonstrated that the aggregation occurs on a macromolecular level, as evidenced by the formation of high molecular weight (HMW) species with conjugates **8–11** which were clearly observable by chromatography (Table 2). Aggregates were formed only in those conjugates which were labeled with non-PEGylated dye. Furthermore, the degree of aggregation is directly related to the amount of dye loaded onto the protein. Interestingly, previous studies which describe the synthesis of ICG-mAb conjugates fail to report any SE-HPLC data, stating only that purification of the conjugation reaction mixture involved elution through a desalting PD-10 column (24,26–32) to remove any excess or unreacted dye. However, this method is incapable of discriminating between the labeled mAb and any aggregates. The assumptions were that the eluted fraction was a pure product. The SE-HPLC analysis presented in this study demonstrates that this assumption cannot be made. The SE-HPLC data clearly demonstrates that the PEGylated conjugates (**12–14**) were void of aggregate formation. Indeed, it has been reported many times in the literature that PEGylation of mAbs and mAb fragments is useful in preventing their aggregation in solution (35).

To determine if aggregation was an equilibrium-based process, conjugate **8** was purified by SE-HPLC, the aggregate was separated from the IgG fraction, the corresponding fractions pooled together and concentrated. Measurement of absorption spectra in PBS confirmed their identities (Figure 5). These repurified products were allowed to sit at 4 °C for three weeks, after which time an aliquot was taken and characterized by SE-HPLC. No formation of aggregates was observed, suggesting that the bioconjugate is stable, and that therefore the observed aggregation is not an equilibrium based process but a result of the amount of dye loaded in the conjugation reaction.

All bioconjugates under study were analyzed by SDS-PAGE under both non-denaturing (Figure 6a) and denaturing (Figure 6b) conditions. Under non-denaturing conditions, the band patterns for conjugates **6 – 11** suggest that the presence of SDS was sufficient to disassociate any aggregates present. Furthermore, since all samples under study exhibit the

same band pattern as that of native panitumumab in the presence of β-ME, it can be inferred that the aggregates observed in SE-HPLC are associated purely by supramolecular forces; i.e. no covalent cross-linking between antibody molecules during the conjugation reaction occurred. A slight smearing of bands is observed for the PEGylated compounds **12 – 14** under both conditions, a behavior observed previously in other PEGylated antibodies and antibody fragments (35).

The SDS-PAGE data suggest that the mechanism of fluorescence activation previously described for other ICG-labeled mAbs *in vitro* in the presence of 5% SDS and β-ME or upon cell internalization, and *in vivo* with mouse cancer xenografts (31–32), could actually be the result of dye disaggregation of the dye-mAb conjugate. On the other hand, no such problem is anticipated for PEGylated compounds **12** – **14** as they form no aggregates; furthermore, the linear polymer can serve as an effective spacer to minimize dye-dye interactions.

PEGylated mAbs **12** – **14** were analyzed by competition radioimmunoassay against ^{125}I-labeled panitumumab (Figure 7). The amount of bioconjugate required for 50% inhibition increased with the degree of labeling: 14 ng (**12**), 15 ng (**13**), 23 ng (**14**) vs. 10 ng (native panitumumab). Though **12** and **13** exhibit comparable affinities, **14** showed the least amount of affinity among the samples under study, indicating a threshold value had been reached. Therefore, modification of panitumumab with **5** with a resulting D/P ratio less than 3 did not significantly compromise the immunoreactivity of the mAb.

Finally, **12** and **15** (negative control) were used to stain HER-1 expressing A431 cells and their fluorescence monitored by confocal microscopy. The images taken of fixed cells show that the panitumumab-based bioconjugate binds to the cell membranes (Figure 8). Fluorescence of the probe is observed even without internalization into the cell. This reinforces the previously described mechanism of fluorescence activation upon internalization into cells to be one of disaggregation of the dye-mAb conjugate. Fluorescence images of viable cells were also taken and showed similar binding of the fluorescent probe to the cell membranes (Supplementary Figure 5).

In summary, a PEGylated amine-reactive derivative of NIR-emitting cyanine dye ICG has been successfully synthesized. This was used to label the anti-HER1 antibody panitumumab, and the resulting bioconjugate was characterized alongside previously reported non-PEGylated analogues. UV-Vis spectrophotometry and SE-HPLC demonstrate that PEGylation prevents aggregation of the bioconjugate from occurring, in comparison with the non-PEGylated analogues. SDS-PAGE analysis of the bioconjugates show that the presence of SDS is sufficient to disassociate any aggregates formed, and denaturation with β-ME also shows that aggregation is not the result of covalent cross-linkage. These results suggest that the previously reported mechanism of fluorescence activation in ICG-labeled mAbs probably occurs via dye disaggregation. Competitive radioimmunoassay demonstrated that PEGylation of panitumumab with 2 equivalents of **5** did not significantly reduce immunoreactivity of the mAb. This result was demonstrated further by fluorescence microscopy of HER1-expressing A431 cells stained with the PEGylated mAb, showing fluorescence on the cell membrane without internalization. This study highlights the fact that, though many protocols for the purification of bioconjugates are well-established and tools for these are commercially available as kits, the need to thoroughly characterize novel bioconjugates using classical methods is necessary to have a proper understanding of their solution properties and speciation.

It is hoped that the PEGylated bioconjugates described here would exhibit not only improved fluorescence properties *in vivo* but also better pharmacokinetic behavior in visualizing HER1-expressing tumor lesions. Indeed the benefits of PEGylating proteins for

therapeutic purposes have been described thoroughly in the literature, namely, that PEGylation increases the *in vivo* circulation half-life of the protein thereby enhancing its bioavailability, and that the modified protein exhibits a reduced immunogenicity and antigenicity coupled with increased plasma stability as the steric hindrance introduced by the water-soluble polymer masks it from proteolytic enzymes and other degrading agents (45–47). Hence, future work involving these single-modality imaging agents will include *in vivo* testing in animal models to determine their biodistribution and other pharmacokinetic characteristics. Futhermore, it is of immediate interest to this group to assess if PEGylation will improve the solution and *in vivo* biodistribution properties of our previously reported dual-modality optical/SPECT imaging agents (18–19), as PEGylation of a radiolabeled protein for SPECT imaging has previously been shown to possess improved pharmacokinetic behavior in the non-invasive monitoring of tumor response to applied therapy (48).

Supplementary Material

Refer to Web version on PubMed Central for supplementary material.

Acknowledgments

This research was supported by the Intramural Research Program of the NIH, National Cancer Institute, Center for Cancer Research. We would like to acknowledge the assistance of Dr. Kwamena Baidoo for supplying the ^{125}I-labeled panitumumab for the radioimmunoassay and Dr. Hisataka Kobayashi for the use of the confocal fluorescence microscope.

References

1. Weissleder R, Ntziachristos V. Shedding light onto live molecular targets. Nat Med. 2003; 9:123–128. [PubMed: 12514725]
2. Frangioni JV. *In vivo* near-infrared fluorescence imaging. Curr Opin Chem Biol. 2003; 7:626–634. [PubMed: 14580568]
3. Hilderbrand SA, Weissleder R. Near-infrared fluorescence: application to *in vivo* molecular imaging. Curr Opin Chem Biol. 2010; 14:71–79. [PubMed: 19879798]
4. Ernst LA, Gupta RK, Mujumdar RB, Waggoner AS. Cyanine dye labeling reagents for sulfhydryl groups. Cytometry. 1989; 10:3–10. [PubMed: 2917472]
5. Mujumdar RB, Ernst LA, Mujumdar SR, Waggoner AS. Cyanine dye labeling reagents containing isothiocyanate groups. Cytometry. 1989; 10:11–19. [PubMed: 2917470]
6. Southwick PL, Ernst LA, Tauriello EW, Parker SR, Mujumdar RB, Mujumdar SR, Clever HA, Waggoner AS. Cyanine dye labeling reagents -carboxymethylindocyanine succinimidyl esters. Cytometry. 1990; 11:418–430. [PubMed: 2340776]
7. Mujumdar RB, Ernst LA, Mujumdar SR, Lewis CJ, Waggoner AS. Cyanine dye labeling reagents: sulfoindocyanine succinimidyl esters. Bioconjugate Chem. 1993; 4:105–111.
8. Mujumdar SR, Mujumdar RB, Grant CM, Waggoner AS. Cyanine-labeling reagents: sulfobenzindocyanine succinimidyl esters. Bioconjugate Chem. 1996; 7:356–362.
9. Gruber HJ, Hahn CD, Kada G, Riner CK, Harms GS, Ahrer W, Dax TG, Knaus HG. Anomalous fluorescence enhancement of Cy3 and Cy3.5 versus anomalous fluorescence loss of Cy5 and Cy7 upon colvaent linking to IgG and noncovalent binding to avidin. Bioconjugate Chem. 2000; 11:696–704.
10. Berlier JE, Rothe A, Buller G, Bradford J, Gray DR, Filanoski BJ, Telford WG, Yue S, Liu J, Cheung CY, Chang W, Hirsch JD, Beechem JM, Haugland RP, Haugland RP. Quantitative comparison of long-wavelength Alexa Fluor dyes to Cy dyes: fluorescence of the dyes and their bioconjugates. J Histochem Cytochem. 2003; 51:1699–1712. [PubMed: 14623938]
11. Lin Y, Weissleder R, Tung CH. Novel near-infrared cyanine fluorochromes: synthesis, properties and bioconjugation. Bioconjugate Chem. 2002; 13:605–610.

12. Hilderbrand SA, Kelly KA, Weisledder R, Tung CH. Monofunctional near-infrared fluorochromes for imaging applications. Bioconjugate Chem. 2005; 16:1275–1281.
13. Bouteiller C, Clave G, Bernardin A, Chipon B, Massonneau M, Renard PY, Romieu A. Novel water-soluble near-infrared cyanine dyes: synthesis, spectral properties and use in the preparation of internally-quenched fluorescent probes. Bioconjugate Chem. 2007; 18:1303–1317.
14. Ballou B, Fisher GW, Deng JS, Hakala TR, Srivastava M, Farkas DL. Cyanine fluorochrome-labeled antibodies *in vivo*: assessment of tumor imaging using Cy3, Cy5, Cy5.5 and Cy7. Cancer Detect Prev. 1998; 22:251–257. [PubMed: 9618048]
15. Zou P, Xu S, Povoski SP, Wang A, Johnson MA, Martin EW, Subramaniam V, Xu R, Sun D. Near-infrared fluorescence labeled anti-TAG-72 monoclonal antibodies for tumor imaging in colorectal cancer xenograft mice. Molec Pharm. 2009; 6:428–440. [PubMed: 19718796]
16. Ogawa M, Regino CAS, Choyke PL, Kobayashi H. *In vivo* target-specific activatable near-infrared optical labeling of humanized monoclonal antibodies. Mol Cancer Ther. 2009; 8:232–239. [PubMed: 19139133]
17. Rosenthal EL, Kulbersh BD, Duncan RD, Zhang W, Magnuson JS, Carroll WR, Zinn K. *In vivo* detection of head and neck cancer orthotopic xenografts by immunofluorescence. Laryngoscope. 2006; 116:1636–1641. [PubMed: 16954995]
18. Xu H, Baidoo K, Gunn AJ, Boswell A, Milenic DE, Choyke PL, Brechbiel MW. Design, synthesis and characterization of a dual modality positron emission tomography and fluorescence imaging agent for monoclonal antibody tumor-targeted imaging. J Med Chem. 2007; 50:4759–4765. [PubMed: 17725340]
19. Xu H, Eck PK, Baidoo KE, Choyke PL, Brechbiel MW. Toward preparation of antibody-based imaging probe libraries for dual modality positron emission tomography and fluorescence imaging. Bioorg Med Chem. 2009; 17:5176–5181. [PubMed: 19505829]
20. Fox IJ, Brooker LGS, Heseltine DW, Essez HE, Wood EH. A tricarbocyanine dye for continuous recording of dilution curves in whole blood independent of variations in blood oxygen saturation. Proc Staff Meet Mayo Clin. 1957; 32:478–484. [PubMed: 13465828]
21. Fox IJ, Wood EH. Indocyanine green: physical and physiologic properties. Proc Staff Meet Mayo Clin. 1960; 35:732–744. [PubMed: 13701100]
22. Landsman MLJ, Kwant G, Mook GA, Zijlstra WG. Light-absorbing properties, stability and spectral stabilization of indocyanine green. J Appl Physiol. 1976; 40:575–583. [PubMed: 776922]
23. Philip R, Penzkofer A, Baumler W, Szeimies RM, Abels C. Absorption and fluorescence spectroscopic investigation of indocyanine green. J Photochem Photobiol A. 1996; 96:137–148.
24. Ito S, Muguruma N, Kakehashi Y, Hayashi S, Okamura S, Shibata H, Okahisa T, Kanamori M, Takesako K, Nozawa M, Ishida K, Shiga M. Development of fluorescence-emitting antibody labeling substance by near-infrared ray excitation. Bioorg Med Chem Lett. 1995; 5:2689–2694.
25. Hirata T, Kogiso H, Morimoto K, Miyamoto S, Taue H, Sano S, Muguruma N, Ito S, Nagao Y. Synthesis and reactivities of 3-indocyanine-green-acyl-1,3-thiazolidine-2-thione (ICG-ATT) as a new near-infrared fluorescent-labeling reagent. Bioorg Med Chem. 1998; 6:2179–2184. [PubMed: 9881108]
26. Muguruma N, Ito S, Hayashi S, Taoka S, Kakehashi Y, Ii K, Shibamura S, Takesako K. Antibodies labeled with fluorescence-agent excitable by infrared rays. J Gastroenterol. 1998; 33:467–471. [PubMed: 9719226]
27. Tadatsu M, Ito S, Muguruma N, Kusaka Y, Inayama K, Bando T, Tadatsu Y, Okamoto K, Ii K, Nagao Y, Sano S, Taue H. A new infrared fluorescent-labeling agent and labeled antibody for diagnosis microcancers. Bioorg Med Chem. 2003; 11:3289–3294. [PubMed: 12837539]
28. Tadatsu Y, Muguruma N, Ito S, Tadatsu M, Kusaka Y, Okamoto K, Imoto Y, Taue H, Sano S, Nagao Y. Optimal labeling condition of antibodies available for immunofluorescence endoscopy. J Med Invest. 2006; 53:52–60. [PubMed: 16537996]
29. Yano H, Muguruma N, Ito S, Aoyagi E, Kimura T, Imoto Y, Cao J, Inoue S, Sano S, Nagao Y, Kido H. Fab fragment labeled with ICG-derivative for detecting digestive tract cancer. Photodiagnosis Photodyn Ther. 2006; 3:177–183.

30. Withrow KP, Gleysteen JP, Safavy A, Skipper J, Desmond RA, Zinn K, Rosenthal EL. Assessment of indocyanine green-labeled cetuximab to detect xenografted head and neck cancer cell lines. Otolaryngol Head Neck Surg. 2007; 137:729–734. [PubMed: 17967636]
31. Ogawa M, Kosaka N, Choyke PL, Kobayashi H. *In vivo* molecular imaging of cancer with a quenching near-inrared fluorescent probe using conjugates of monoclinal antibodies and indocyanine green. Cancer Res. 2009; 69:1268–1272. [PubMed: 19176373]
32. Ogawa M, Regino CAS, Seidel J, Green MV, Xi W, Williams M, Kosaka N, Choyke PL, Kobayashi H. Dual-modality molecular imaging using antibodies labeled with activatable fluorescence and a radionuclide for specific and quantitative targeted cancer detection. Bioconjugate Chem. 2009; 20:2177–2184.
33. Yarden Y, Sliwkowski MX. Untangling the ErbB signalling network. Nat Rev Mol Cell Biol. 2001; 2:127–137. [PubMed: 11252954]
34. Zalipsky S. Chemistry of polyethylene glycol conjugates with biologically active molecules. Adv Drug Del Rev. 1995; 16:157–182.
35. Chapman AP. PEGylated antibodies and antibody fragments for improved therapy: a review. Adv Drug Del Rev. 2002; 54:531–545.
36. Millar WT, Smith JFB. Protein iodination using Iodogen^{R}. Int J Appl Radiat Isot. 1983; 34:639–641. [PubMed: 6343255]
37. Laemmli UK. Cleavage of structural proteins during the assembly of the head of Bacteriophage T4. Nature. 1970; 227:680–685. [PubMed: 5432063]
38. Nagao Y, Seno K, Kawabata K, Miyasaka T, Takao S, Fujita E. Monitored aminolysis of 3-acylthiazolidine-2-thione: a new convenient synthesis of amide. Tetrahedron Lett. 1980; 21:841–844.
39. Nagao Y, Seno K, Miyasaka T, Fujita E. Monitored aminolysis of 3- acylthiazolidine-2-thione: a new synthesis of macrocyclic amides. Chem Lett. 1980; 9:159–162.
40. Baker KJ. Binding of sulfobromophthalein (BSP) sodium and indocyanine green (ICG) by plasma α_1 lipoproteins. Proc Soc Exptl Biol Med. 1962; 122:957–963. [PubMed: 5918158]
41. West W, Pearce S. The dimeric state of cyanine dyes. J Phys Chem. 1965; 69:1894–1903.
42. Benson RC, Kues HA. Fluorescence properties of indocyanine green as related to angiography. Phys Med Biol. 1978; 23:159–163. [PubMed: 635011]
43. McKinney RM, Spillane JT. An approach to quantitation in rhodamine isothiocyanate labeling. Ann N Y Acad Sci. 1975; 254:55–64. [PubMed: 52324]
44. Chen RF. Fluorescent protein-dye conjugates II. Gamma globulin conjugated with various dyes. Arch Bioch Biophys. 1969; 133:263–276.
45. Fuertges F, Abuchowski A. The clinical efficacy of poly(ethylene glycol)-modified proteins. J Control Release. 1990; 11:139–148.
46. Chapman AP, Antoniw P, Spitali M, West S, Stephens S, King DJ. Therapeutic antibody fragments with prolonged in vivo half–lives. Nat Biotechnol. 1999; 17:780– 783. [PubMed: 10429243]
47. Veronese FM, Pasut G. PEGylation, successful approach to drug delivery. Drug Discov Today. 2005; 10:1451 – 1458. [PubMed: 16243265]
48. Wen X, Wu QP, Ke S, Wallace S, Charnsangavej C, Huang P, Liang D, Chow D, Li C. Improved radiolabeling of PEGylated protein: PEGylated annexin V for non-invasive imaging of tumor apoptosis. Cancer Biother Radio. 2003; 18:819–827.

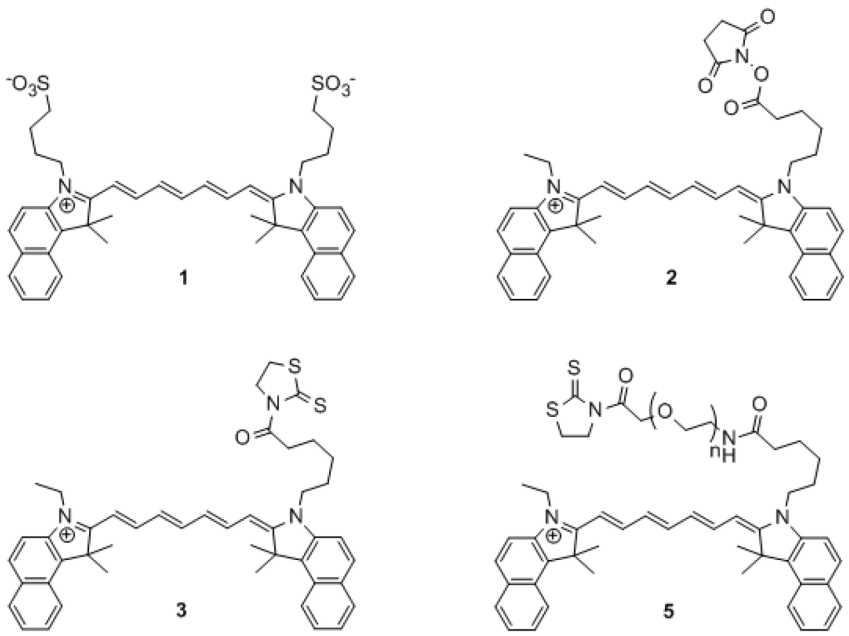

Figure 1.
(**1**) ICG, (**2**) ICG-OSu, (**3**) ICG-ATT, (**5**) ICG-PEG-ATT

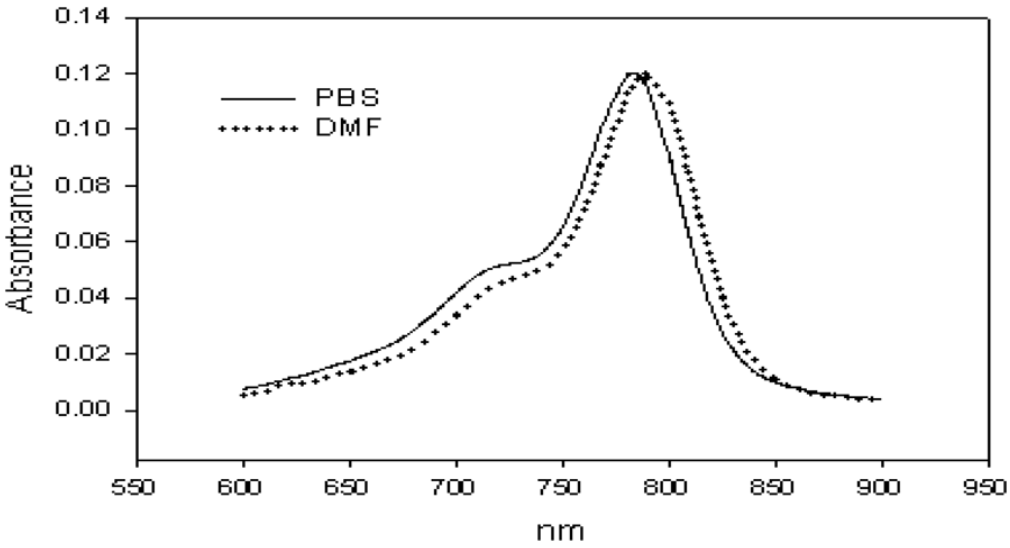

Figure 2.
A slight red shift in the λ_{max} of **5** is observed when in aqueous solvent (PBS) vs. organic solvent (DMF).

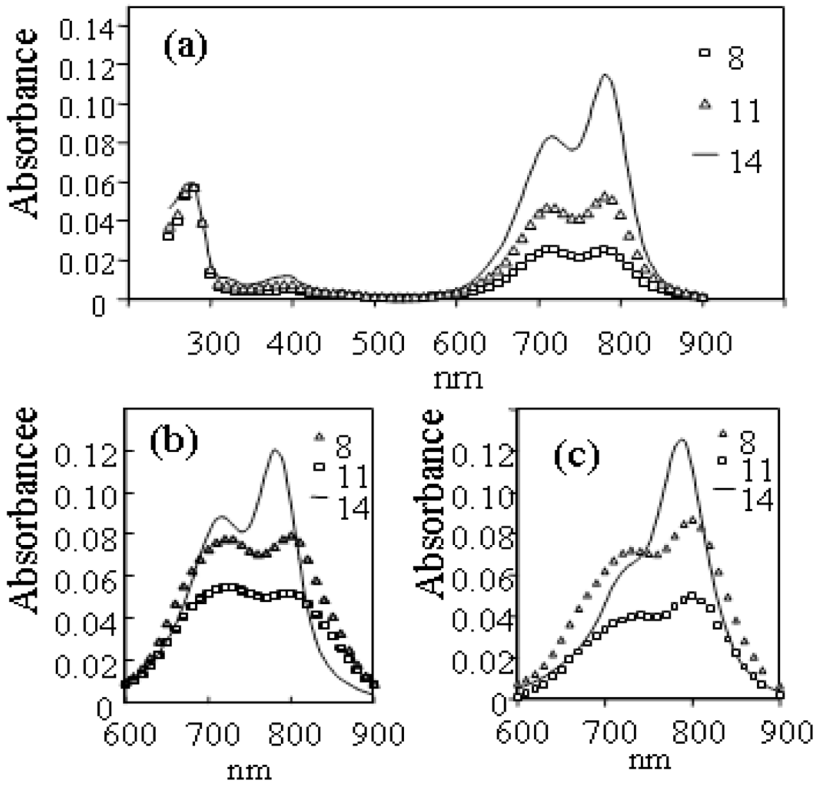

Figure 3.
(a) ICG-PEG-mAbs **12**, **13**, **14** in PBS, (b) **8**, **11**, **14** in PBS, (c) **8**, **11**, **14** in 9:1 PBS:DMF (50 μg samples).

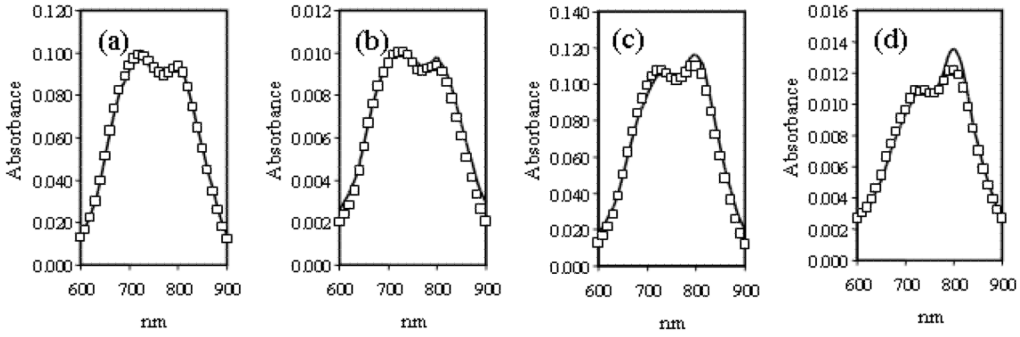

Figure 4.

(a) and (b) **11** in PBS, (c) and (d) **11** in 2:8 DMSO:PBS at (□) 0.5 mg/mL and (−) 0.1 mg/mL.

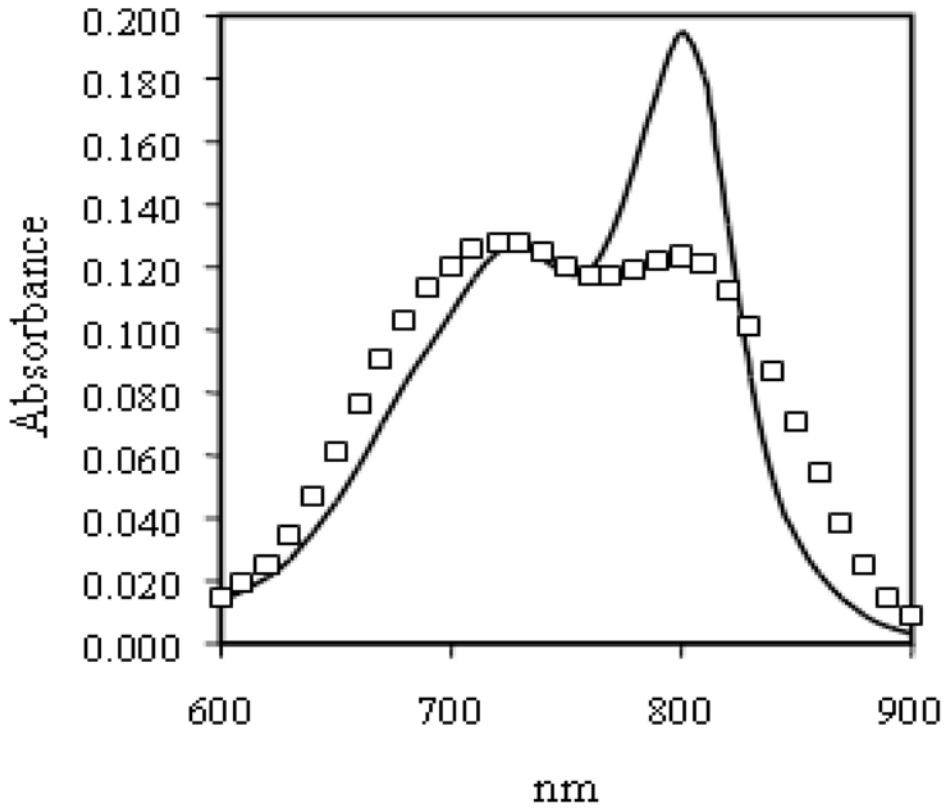

Figure 5.
Absorption spectra of (□) aggregate HMW fraction and (—) pure IgG fraction.

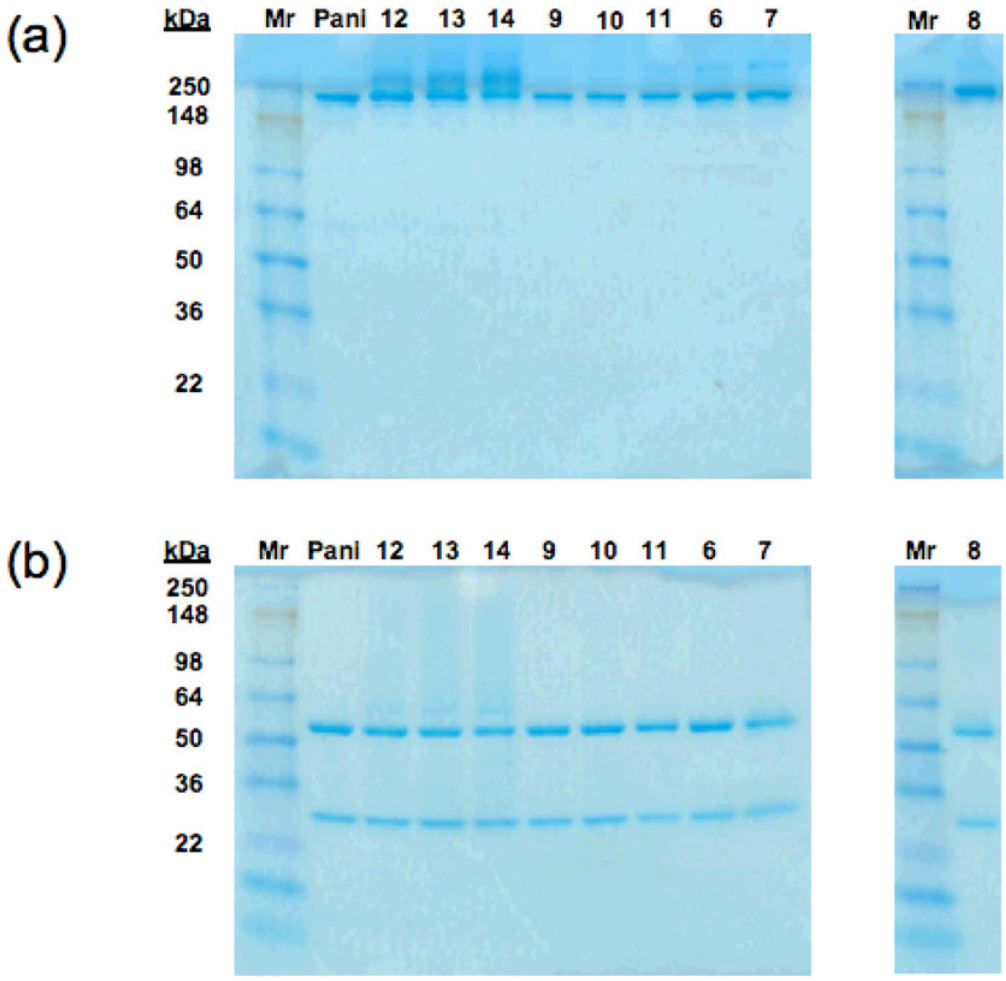

Figure 6.
SDS-PAGE of ICG-labeled panitumumab bioconjugates under (a) non-denaturing and (b) denaturing conditions with β-ME.

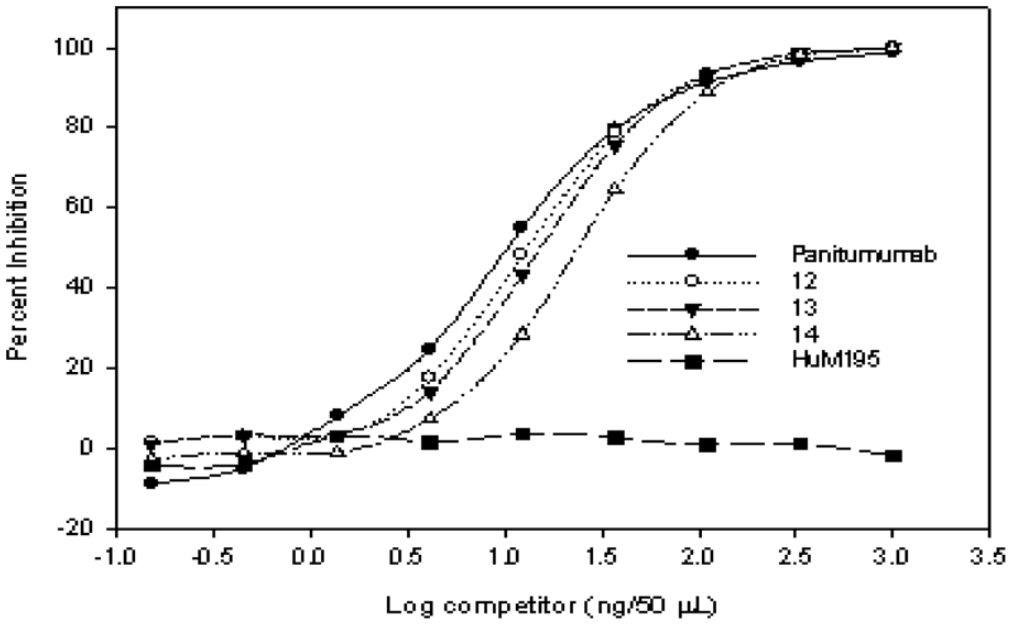

Figure 7.
Competition RIA of **12**, **13** and **14** with ^{125}I-Panitumumab

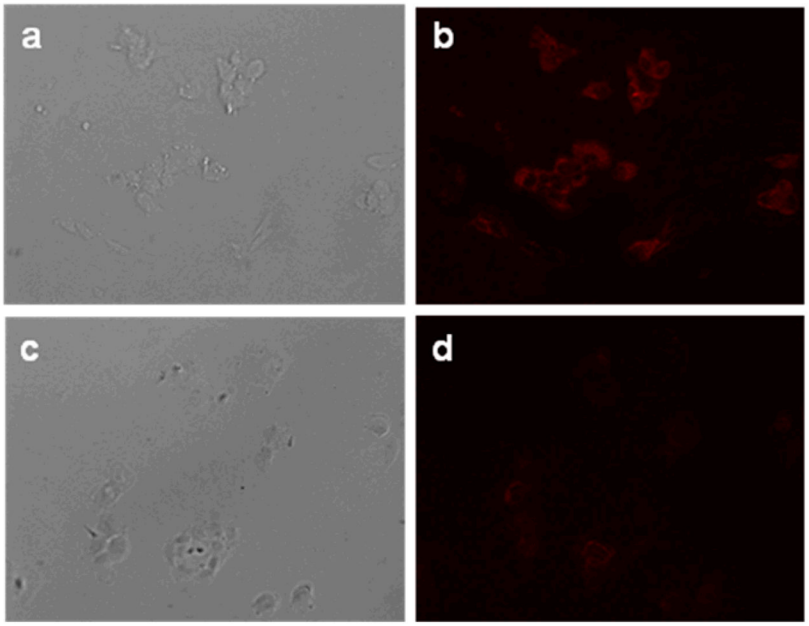

Figure 8.
HER1-positive A431 fixed cells incubated with 1μg of test antibody for 1 h at 37 °C. (a) DIC and (b) fluorescence image of cells stained with **12**. (c) DIC and (d) fluorescence image of cells stained with **15** (negative control).

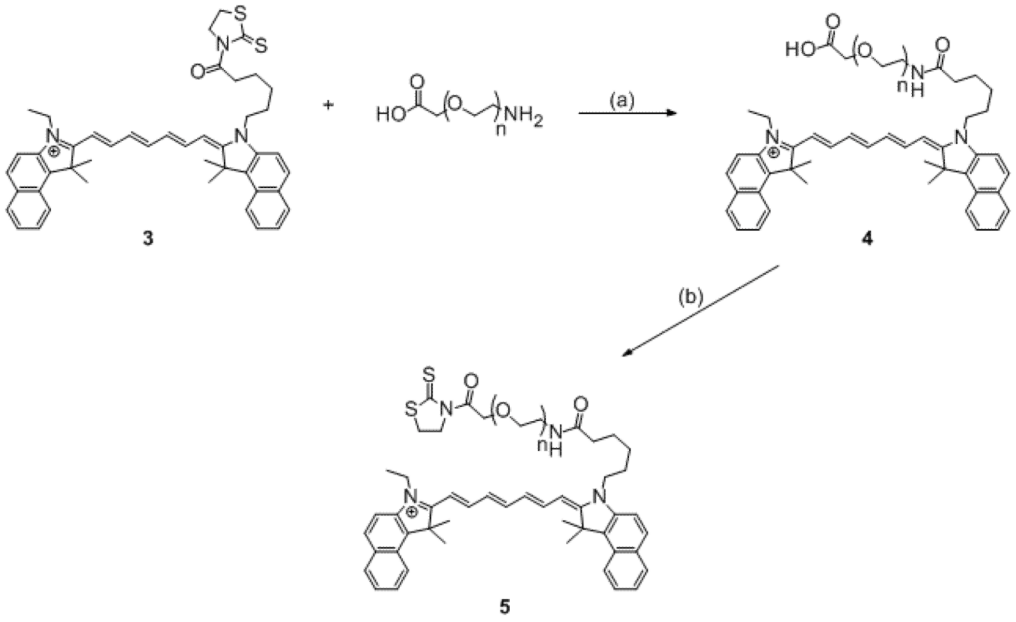

Scheme 1.
Synthesis of **5**: (a) Et_3N, MeCN, 0 °C, (b) DCM, EDC, DMAP, ATT, 0 °C.

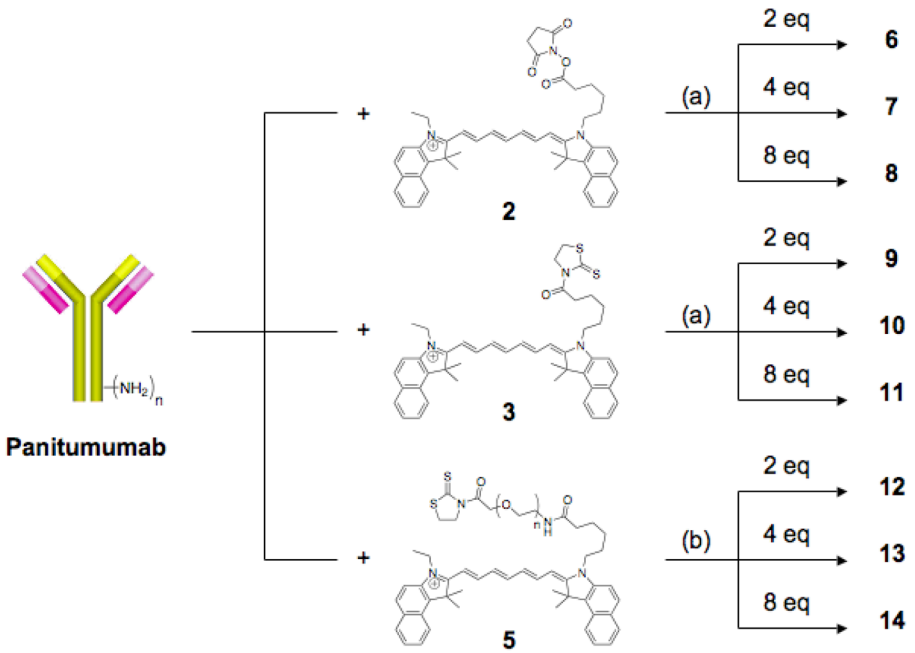

Scheme 2.

Conjugation of **2**, **3** and **5** with panitumumab: (a) 25% DMSO in 0.1 M $NaHCO_3$ buffer, (b) 0.1 M $NaHCO_3$ buffer.

Table 1

Comparison of optical properties of 3 and 5 in different solvents.

	Compound			
	3		5	
Solvent	**λ_{max}**	**ε(μM^{-1} cm^{-1})**	**λ_{max}**	**ε(μM^{-1} cm^{-1})**
PBS	---	---	783	0.155
9:1 PBS:DMF	800	0.034	785	0.154
DMF	790	0.170	790	0.158

Table 2

SE-HPLC data of conjugates

Sample	% HMW	% IgG
6	9.2	90.8
7	15.7	84.3
8	26.0	74.0
9	5.3	94.7
10	12.2	87.9
11	19.9	74.0
12	0	100
13	0	100
14	0	100

IgG (Panitumumab): t_R = 19.9 min; HMW species (**6**–**8**): t_R = 11.2 and 16.9–18.4 min; HMW (**9**–**11**): t_R = 11.2; molecular weight standards: 158 kDa (20.5 min), 232 kDa (19.3 min), 440 kDa (16.5 min), Blue Dextran (11.2 min).